The POG Technique for Modeling Planetary Gears and Hybrid Automotive Systems

Roberto Zanasi
Information Engineering Department
University of Modena e Reggio Emilia
Via Vignolese 905
41100 Modena, Italy
roberto.zanasi@unimore.it

Federica Grossi
Information Engineering Department
University of Modena e Reggio Emilia
Via Vignolese 905
41100 Modena, Italy
federica.grossi@unimore.it

***Abstract*—In this paper the Power-Oriented Graphs (POG) technique is used for modeling planetary gears and hybrid automotive systems. Some basic properties of the POG technique are firstly given. An extended dynamic model of a planetary gear with internal elasticity is presented. Then a POG congruent state space transformation is used to transform and reduce the system when the elasticities or the inertias go to zero. The obtained reduced model is used as central element of an hybrid automotive power structure (endothermic engine, multi-phase synchronous motor and vehicle dynamics). Simulation results of the modeled hybrid system ends the paper.**

I. Introduction

Nowadays, the planetary gears are key elements for the design of new hybrid power structures in the automotive area. In this paper, some detailed dynamic models of a planetary gear and an hybrid automotive system are given using the Power-Oriented Graphs (POG) technique. This technique allows to graphically describes the dynamic model of any type of physical system putting in evidence the powers which flow within the modeled systems. The POG schemes are easy to use, easy to understand and can be directly implemented in Simulink. The paper is organized as follows: Sec. II describes the basic properties of the POG modeling technique. Sec. III and Sec. IV show, respectively, the POG dynamic models of full and reduced planetary gears, and of an hybrid automotive power structure composed by an endothermic engine, a multi-phase synchronous motor and the vehicle dynamics. Finally, in Sec. V some simulation results are reported.

II. Power-Oriented Graphs basic principles

The Power-Oriented Graphs technique, see [1] and [2], is suitable for modeling physical systems. The POG block schemes are normal block diagrams combined with a particular modular structure essentially based on the use of the two blocks shown in Fig. 1.a and Fig. 1.b: the *elaboration block* (e.b.) stores and/or dissipates energy (i.e. springs, masses, dampers, capacities, inductances, resistances, etc.); the *connection block* (c.b.) redistributes the power within the system without storing nor dissipating energy (i.e. any type of gear reduction, transformers, etc.). The e.b. and the c.b. are suitable for representing both scalar and vectorial systems. In the vectorial case, $\mathbf{G}(s)$ and $\mathbf{K}$ are matrices: $\mathbf{G}(s)$ is always a square matrix composed by positive real transfer functions; matrix $\mathbf{K}$ can also be rectangular. The circle present in the e.b. is a summation element and the black spot represents a minus sign that multiplies the entering variable. The main feature of the Power-Oriented Graphs is to keep a direct correspondence between the dashed sections of the graphs and real power sections of the modeled systems: the scalar product $\mathbf{x}^{\mathrm{T}}\mathbf{y}$ of the two *power vectors* $\mathbf{x}$ and $\mathbf{y}$ involved in each dashed line of a power-oriented graph, see Fig. 1, has the physical meaning of *the power flowing through that particular section*. The Bond Graphs technique, see [3] and [4], is based on the same idea, but it uses a different and specific graphical representation.

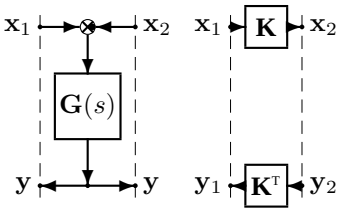

a) *e. b.* b) *c. b.*

	POG Variables	
Domains:	*Across:* v_e	*Through:* v_f
Electrical	Voltage V	Current I
Mec. Tra.	Velocity v	Force F
Mec. Rot.	Ang. Vel. ω	Torque τ
Hydraulic	Pressure P	Flow rate Q

c) *Across and through variables*

Figure 1. POG basic blocks and variables: a) *elaboration block*; b) *connection block*; c) *across and through variables*.

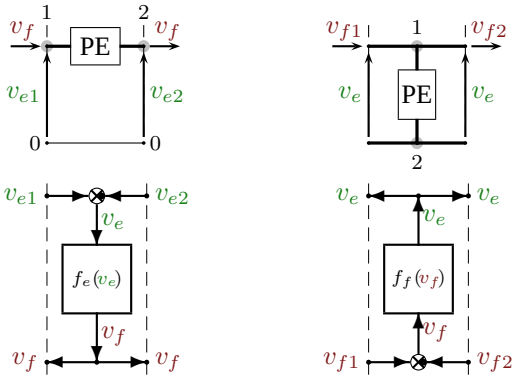

a) Element in series. b) Element in parallel.

Figure 2. POG representations of Physical Elements (PE): a) connected in series (inputs v_{e1}, v_{e2}); b) connected in parallel (inputs v_{f1}, v_{f2}).

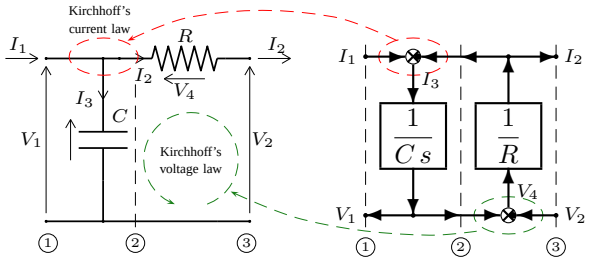

Figure 3. POG modeling of an electrical RC circuit.

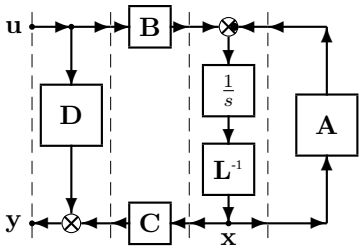

$$\begin{cases} \mathbf{L}\,\dot{\mathbf{x}} = -\mathbf{A}\,\mathbf{x} + \mathbf{B}\,\mathbf{u} \\ \mathbf{y} = \mathbf{C}\,\mathbf{x} + \mathbf{D}\,\mathbf{u} \end{cases} \tag{1}$$

$$\Downarrow (\mathbf{x} = \mathbf{T}\,\mathbf{z})$$

$$\begin{cases} \overline{\mathbf{L}}\,\dot{\mathbf{z}} = -\overline{\mathbf{A}}\,\mathbf{z} + \overline{\mathbf{B}}\,\mathbf{u} \\ \mathbf{y} = \overline{\mathbf{C}}\,\mathbf{z} + \overline{\mathbf{D}}\,\mathbf{u} \end{cases} \tag{2}$$

Figure 4. POG block scheme of a generic dynamic system.

The main energetic domains encountered in modeling physical systems are the electrical, the mechanical (translational and rotational) and the hydraulic, see Fig. 1.c. Each energetic domain is characterized by two *power variables*: an *across-variable* v_e defined between two points (i.e. the voltage V, the velocity $\dot{x}$, etc.), and a *through-variable* v_f defined in each point of the space (i.e. the current I, the force F, etc.). Each Physical Element (PE) interacts with the external world through the power sections associated to its terminals. A Physical Element is connected *in series* when its terminals share the same through-variable v_f: see the physical element and the corresponding POG scheme in Fig. 2.a. A Physical Element is connected *in parallel* when its terminals share the same across-variable v_e: see the physical element and the POG scheme in Fig. 2.b. An example of POG modeling is shown in Fig. 3 where a C-parallel element is connected with an R-series element. There is a direct correspondence between physical power sections and dashed sections in the POG model. Note: the summation elements present in the elaboration blocks are a mathematical description of the current and voltage Kirchhoff's laws applied to the considered electrical system.

Another important property of the POG technique is the direct correspondence between the POG schemes and the corresponding state space dynamic equations. For example, the POG scheme shown in Fig. 4 can be represented by the state space equations (1) where the *energy matrix* $\mathbf{L}$ is symmetric and positive definite: $\mathbf{L} = \mathbf{L}^{\mathrm{T}} > 0$. It can be easily shown that when $\mathbf{D} = 0$ it follows that $\mathbf{C} = \mathbf{B}^{\mathrm{T}}$. When an eigenvalue of matrix $\mathbf{L}$ tends to zero (or to infinity), system (1) degenerates towards a lower dimension dynamic system. In this case, the dynamic model of the "reduced" system, see (2), can be directly obtained from (1) using a simple "congruent" transformation $\mathbf{x} = \mathbf{T}\,\mathbf{z}$ where (if $\mathbf{T}$ is constant) $\overline{\mathbf{L}} = \mathbf{T}^{\mathrm{T}}\mathbf{L}\mathbf{T}$, $\overline{\mathbf{A}} = \mathbf{T}^{\mathrm{T}}\mathbf{A}\mathbf{T}$, $\overline{\mathbf{B}} = \mathbf{T}^{\mathrm{T}}\mathbf{B}$, $\overline{\mathbf{C}} = \mathbf{C}\mathbf{T}$ and $\overline{\mathbf{D}} = \mathbf{D}$. The POG scheme of Fig. 4 can also be easily input-output inverted, both graphically and mathematically, as shown in Fig. 5. In this case $\tilde{\mathbf{L}} = \mathbf{L}$, $\tilde{\mathbf{A}} = \mathbf{A} + \mathbf{B}\mathbf{D}^{-1}\mathbf{C}$, $\tilde{\mathbf{B}} = \mathbf{B}\mathbf{D}^{-1}$, $\tilde{\mathbf{C}} = -\mathbf{D}^{-1}\mathbf{C}$ and $\tilde{\mathbf{D}} = \mathbf{D}^{-1}$ are the matrices of the inverted system (3).

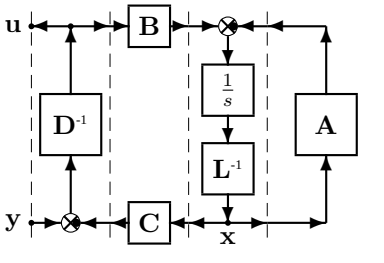

$$\begin{cases} \tilde{\mathbf{L}}\,\dot{\mathbf{x}} = -\tilde{\mathbf{A}}\,\mathbf{x} + \tilde{\mathbf{B}}\,\mathbf{y} \\ \mathbf{u} = \tilde{\mathbf{C}}\,\mathbf{x} + \tilde{\mathbf{D}}\,\mathbf{y} \end{cases} \tag{3}$$

where

$$\tilde{\mathbf{L}} = \mathbf{L}, \quad \tilde{\mathbf{B}} = \mathbf{B}\mathbf{D}^{-1},$$
$$\tilde{\mathbf{A}} = \mathbf{A} + \mathbf{B}\mathbf{D}^{-1}\mathbf{C},$$
$$\tilde{\mathbf{C}} = -\mathbf{D}^{-1}\mathbf{C}, \quad \tilde{\mathbf{D}} = \mathbf{D}^{-1}.$$

Figure 5. POG block scheme of the input-output inverted system.

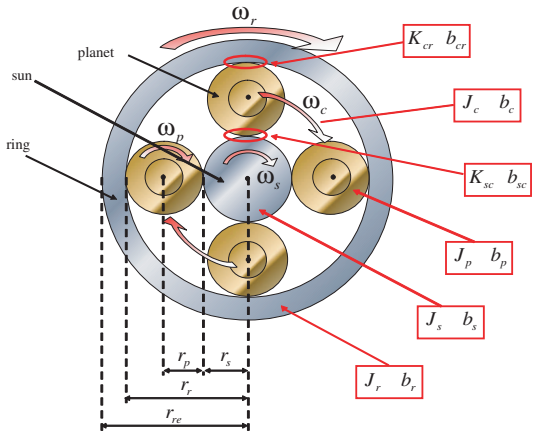

Figure 6. Planetary gear and related parameters.

III. POG MODELING OF A PLANETARY GEAR

Let us consider the planetary gear shown in Fig. 6. The main parameters of the system are: r_s and r_p are the sun and planet radii; J_s, b_s, J_c, b_c, J_r and b_r are the inertia and linear friction coefficients of the sun, carrier and ring, respectively; K_{sc}, d_{sc}, K_{cr} and d_{cr} are the stiffness and friction coefficients of the sun-carrier and carrier-ring elastic elements, respectively. The extended POG dynamic model of the considered planetary gear is shown in the upper part of Fig. 7: the carrier, the planets and the ring interact each other through the two elastic elements K_{cr} and K_{sc}. The corresponding state space dynamic equations are shown in lower part of Fig. 7:

$$\overline{\mathbf{L}}\,\dot{\overline{\mathbf{x}}} = -\overline{\mathbf{A}}\,\overline{\mathbf{x}} + \overline{\mathbf{B}}\,\mathbf{u}, \qquad \mathbf{y} = \overline{\mathbf{B}}^{\mathrm{T}}\overline{\mathbf{x}} \tag{5}$$

The POG linear systems described in form (5) always satisfy the following properties:

1) the energy E_s stored in the system and the dissipating power P_d are quadratic functions of matrices $\overline{\mathbf{L}}$ and $\overline{\mathbf{A}}_s$, respectively:

$$E_s = \frac{1}{2}\,\overline{\mathbf{x}}^{\mathrm{T}}\,\overline{\mathbf{L}}\,\overline{\mathbf{x}}, \qquad P_d = \overline{\mathbf{x}}^{\mathrm{T}}\,\overline{\mathbf{A}}_s\,\overline{\mathbf{x}}$$

where $\overline{\mathbf{A}}_s = (\overline{\mathbf{A}} + \overline{\mathbf{A}}^{\mathrm{T}})/2$ is the symmetric part of the *power matrix* $\overline{\mathbf{A}}$. The skew-symmetric part $\overline{\mathbf{A}}_w = (\overline{\mathbf{A}} - \overline{\mathbf{A}}^{\mathrm{T}})/2$ of

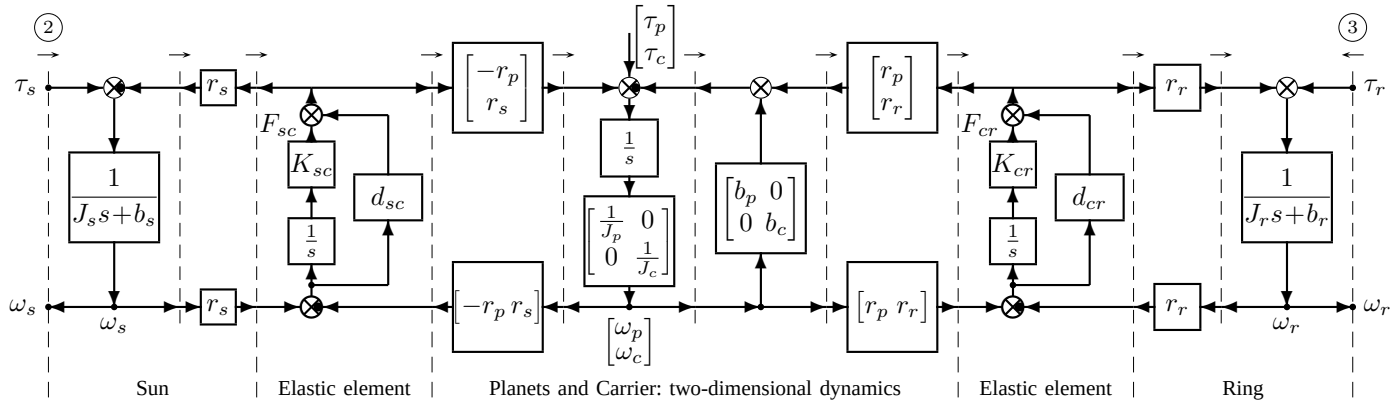

$$\underbrace{\begin{bmatrix} J_s & 0 & 0 & 0 & 0 & 0 \\ 0 & \frac{1}{K_{sc}} & 0 & 0 & 0 & 0 \\ 0 & 0 & J_p & 0 & 0 & 0 \\ 0 & 0 & 0 & J_c & 0 & 0 \\ 0 & 0 & 0 & 0 & \frac{1}{K_{cr}} & 0 \\ 0 & 0 & 0 & 0 & 0 & J_r \end{bmatrix}}_{\overline{\mathbf{L}}} \underbrace{\begin{bmatrix} \dot{\omega}_s \\ \dot{F}_{sc} \\ \dot{\omega}_p \\ \dot{\omega}_c \\ \dot{F}_{cr} \\ \dot{\omega}_r \end{bmatrix}}_{\dot{\overline{\mathbf{x}}}} = \underbrace{\begin{bmatrix} -b_s - r_s^2 d_{sc} & -r_s & -r_s d_{sc} r_p & r_s^2 d_{sc} & 0 & 0 \\ r_s & 0 & r_p & -r_s & 0 & 0 \\ -r_s d_{sc} r_p & -r_p & -b_p - d_{sc} r_p^2 - d_{cr} r_p^2 & r_s d_{sc} r_p - d_{cr} r_p r_r & -r_p & d_{cr} r_p r_r \\ r_s^2 d_{sc} & r_s & r_s d_{sc} r_p - d_{cr} r_p r_r & -b_c - r_s^2 d_{sc} - d_{cr} r_r^2 & -r_r & d_{cr} r_r^2 \\ 0 & 0 & r_p & r_r & 0 & -r_r \\ 0 & 0 & d_{cr} r_p r_r & d_{cr} r_r^2 & r_r & -b_r - d_{cr} r_r^2 \end{bmatrix}}_{-\overline{\mathbf{A}}} \underbrace{\begin{bmatrix} \omega_s \\ F_{sc} \\ \omega_p \\ \omega_c \\ F_{cr} \\ \omega_r \end{bmatrix}}_{\overline{\mathbf{x}}} + \underbrace{\begin{bmatrix} 1 & 0 & 0 \\ 0 & 0 & 0 \\ 0 & 0 & 0 \\ 0 & 1 & 0 \\ 0 & 0 & 0 \\ 0 & 0 & 1 \end{bmatrix}}_{\overline{\mathbf{B}}} \underbrace{\begin{bmatrix} \tau_s \\ \tau_c \\ \tau_r \end{bmatrix}}_{\mathbf{u}} \quad (4)$$

Figure 7. The POG block diagram and the POG state space equations of the considered planetary gear: the sun, the planets-carrier and the ring interact through elastic elements. The considered inputs are: τ_s, τ_c and τ_r.

matrix $\overline{\mathbf{A}}$ represents the power redistribution within the system. One can easily verify that all the dissipating parameters of the system appear only in matrix $\overline{\mathbf{A}}_s$, while matrix $\overline{\mathbf{A}}_w$ is completely characterized by all the connection parameters;
2) all the loops of the POG schemes *always contain an "odd" number of signs "−"* (i.e. the black spots) in the summation blocks of the loop;
3) the direction of the power flowing through a section is positive if *an "even" number of signs "−" is present along all the paths* which link the input and the output of the section. Note, for example, that in Fig. 7 the power is entering the system in both sections ② and ③.

A. Reduced inertial model

For certain applications the POG model of Fig. 7 can be too much detailed. In these cases it can be of interest to find the reduced model when, for example, the stiffness coefficients K_{cr} and K_{sc} tend to infinity. Applying to system (5) the following congruent transformation:

$$\overline{\mathbf{x}} = \mathbf{T}_1 \, \mathbf{x}, \qquad \text{where} \qquad \mathbf{T}_1 = \begin{bmatrix} 1 & 0 & 0 & 0 & 0 & 0 \\ 0 & 0 & 0 & 0 & 0 & 1 \\ 0 & 0 & 1 & 0 & 0 & 0 \\ 0 & 1 & 0 & 0 & 0 & 0 \\ 0 & 0 & 0 & 0 & 1 & 0 \\ 0 & 0 & 0 & 1 & 0 & 0 \end{bmatrix}.$$

one obtains the following transformed system:

$$\underbrace{\begin{bmatrix} \mathbf{J}_1 & 0 & 0 \\ 0 & \mathbf{J}_2 & 0 \\ 0 & 0 & 0 \end{bmatrix}}_{\mathbf{L}} \underbrace{\begin{bmatrix} \dot{\mathbf{x}}_1 \\ \dot{\mathbf{x}}_2 \\ \dot{\mathbf{x}}_3 \end{bmatrix}}_{\dot{\mathbf{x}}} = \underbrace{\begin{bmatrix} \mathbf{A}_{11} & \mathbf{A}_{12} & \mathbf{A}_{13} \\ \mathbf{A}_{21} & \mathbf{A}_{22} & \mathbf{A}_{23} \\ \mathbf{A}_{31} & \mathbf{A}_{32} & 0 \end{bmatrix}}_{-\mathbf{A}} \underbrace{\begin{bmatrix} \mathbf{x}_1 \\ \mathbf{x}_2 \\ \mathbf{x}_3 \end{bmatrix}}_{\mathbf{x}} + \underbrace{\begin{bmatrix} \mathbf{B}_1 \\ \mathbf{B}_2 \\ 0 \end{bmatrix}}_{\mathbf{B}} \mathbf{u} \quad (6)$$

where $\mathbf{x} = \mathbf{T}_1^{\mathrm{T}} \, \overline{\mathbf{x}}$, $\mathbf{L} = \mathbf{T}_1^{\mathrm{T}} \overline{\mathbf{L}} \, \mathbf{T}_1$, $\mathbf{B} = \mathbf{T}_1^{\mathrm{T}} \, \overline{\mathbf{B}}$, $\mathbf{A} = \mathbf{T}_1^{\mathrm{T}} \overline{\mathbf{A}} \, \mathbf{T}_1$, $\mathbf{y} = \mathbf{B}^{\mathrm{T}} \, \mathbf{x}$ and:

$$\mathbf{x}_1 = \begin{bmatrix} \omega_s \\ \omega_c \end{bmatrix}, \; \mathbf{x}_2 = \begin{bmatrix} \omega_p \\ \omega_r \end{bmatrix}, \; \mathbf{x}_3 = \begin{bmatrix} F_{cr} \\ F_{sc} \end{bmatrix}, \; \mathbf{J}_1 = \begin{bmatrix} J_s & 0 \\ 0 & J_c \end{bmatrix}, \; \mathbf{J}_2 = \begin{bmatrix} J_p & 0 \\ 0 & J_r \end{bmatrix},$$

$$\mathbf{B}_1 = \begin{bmatrix} 1 & 0 & 0 \\ 0 & 1 & 0 \end{bmatrix}, \; \mathbf{B}_2 = \begin{bmatrix} 0 & 0 & 0 \\ 0 & 0 & 1 \end{bmatrix}, \; \mathbf{A}_{11} = \begin{bmatrix} -b_s - r_s^2 d_{sc} & r_s^2 d_{sc} \\ r_s^2 d_{sc} & -b_c - r_s^2 d_{sc} - d_{cr} r_r^2 \end{bmatrix},$$

$$\mathbf{A}_{12} = \begin{bmatrix} -r_s d_{sc} r_p & 0 \\ r_s d_{sc} r_p - d_{cr} r_p r_r & d_{cr} r_r^2 \end{bmatrix}, \mathbf{A}_{13} = \begin{bmatrix} 0 & -r_s \\ -r_r & r_s \end{bmatrix}, \mathbf{A}_{31} = \begin{bmatrix} 0 & r_r \\ r_s & -r_s \end{bmatrix},$$

$$\mathbf{A}_{21} = \begin{bmatrix} -r_s d_{sc} r_p & r_s d_{sc} r_p - d_{cr} r_p r_r \\ 0 & d_{cr} r_r^2 \end{bmatrix}, \qquad \mathbf{A}_{23} = \begin{bmatrix} -r_p & -r_p \\ r_r & 0 \end{bmatrix},$$

$$\mathbf{A}_{22} = \begin{bmatrix} -b_p - d_{sc} r_p^2 - d_{cr} r_p^2 & d_{cr} r_p r_r \\ d_{cr} r_p r_r & -b_r - d_{cr} r_r^2 \end{bmatrix}, \qquad \mathbf{A}_{32} = \begin{bmatrix} r_p & -r_r \\ r_p & 0 \end{bmatrix}.$$

The last equation of system (6) shows an algebraic relation between the state variables: $\mathbf{A}_{31} \, \mathbf{x}_1 + \mathbf{A}_{32} \, \mathbf{x}_2 = 0$. Since matrix $\mathbf{A}_{32}$ is invertible, vector $\mathbf{x}_2$ can be expressed as a function of vector $\mathbf{x}_1$:

$$\mathbf{x}_2 = \begin{bmatrix} \omega_p \\ \omega_r \end{bmatrix} = -\mathbf{A}_{32}^{-1} \, \mathbf{A}_{31} \, \mathbf{x}_1 = \begin{bmatrix} -\frac{r_s}{r_p} & \frac{r_s}{r_p} \\ -\frac{r_s}{r_r} & 1 + \frac{r_s}{r_r} \end{bmatrix} \begin{bmatrix} \omega_s \\ \omega_c \end{bmatrix}$$

Applying to system (6) the following "rectangular" and "congruent" state space transformation:

$$\mathbf{x} = \mathbf{T}_2 \, \mathbf{x}_1, \quad \text{where} \quad \mathbf{T}_2 = \begin{bmatrix} \mathbf{I}_2 \\ -\mathbf{A}_{32}^{-1} \, \mathbf{A}_{31} \\ 0 \end{bmatrix} = \begin{bmatrix} 1 & 0 \\ 0 & 1 \\ -\frac{r_s}{r_p} & \frac{r_s}{r_p} \\ -\frac{r_s}{r_r} & 1 + \frac{r_s}{r_r} \\ 0 & 0 \\ 0 & 0 \end{bmatrix}$$

one obtains the following second order transformed and reduced system:

$$\mathbf{L}_r \, \dot{\mathbf{x}}_1 = -\mathbf{A}_r \, \mathbf{x}_1 + \mathbf{B}_r \, \mathbf{u}, \qquad \mathbf{y} = \mathbf{B}_r^{\mathrm{T}} \mathbf{x}_1, \quad (7)$$

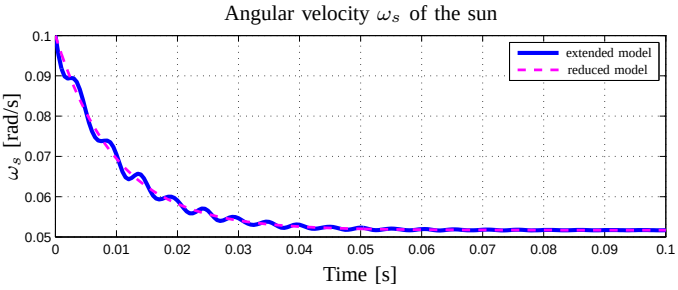

Figure 8. Simulative comparison between the extended (blue solid line) and the reduced (magenta dashed line) model of the planetary gear.

where $\mathbf{L}_r = \mathbf{T}_2^{\mathrm{T}}\mathbf{L}\,\mathbf{T}_2$, $\mathbf{A}_r = \mathbf{T}_2^{\mathrm{T}}\mathbf{A}\,\mathbf{T}_2$ and $\mathbf{B}_r = \mathbf{T}_2^{\mathrm{T}}\,\mathbf{B}$ are:

$$\mathbf{L}_r = \begin{bmatrix} J_s + \frac{r_s^2}{r_p^2}J_p + \frac{r_s^2}{r_r^2}J_r & -\frac{r_s^2}{r_p^2}J_p - \frac{r_s}{r_r}\left(1+\frac{r_s}{r_r}\right)J_r \\ -\frac{r_s^2}{r_p^2}J_p - \frac{r_s}{r_r}\left(1+\frac{r_s}{r_r}\right)J_r & J_c + \frac{r_s^2}{r_p^2}J_p + \left(1+\frac{r_s}{r_r}\right)^2 J_r \end{bmatrix}$$

$$\mathbf{A}_r = \begin{bmatrix} b_s + \frac{r_s^2}{r_p^2}b_p + \frac{r_s^2}{r_r^2}b_r & -\frac{r_s^2}{r_p^2}b_p - \frac{r_s}{r_r}\left(1+\frac{r_s}{r_r}\right)b_r \\ -\frac{r_s^2}{r_p^2}b_p - \frac{r_s}{r_r}\left(1+\frac{r_s}{r_r}\right)b_r & b_c + \frac{r_s^2}{r_p^2}b_p + \left(1+\frac{r_s}{r_r}\right)^2 b_r \end{bmatrix}$$

$$\mathbf{B}_r = \begin{bmatrix} 1 & 0 & -\frac{r_s}{r_r} \\ 0 & 1 & 1+\frac{r_s}{r_r} \end{bmatrix}, \quad \mathbf{x}_1 = \begin{bmatrix} \omega_s \\ \omega_c \end{bmatrix}, \quad \mathbf{y} = \begin{bmatrix} \omega_s \\ \omega_c \\ \omega_r \end{bmatrix}.$$

Note: the possibility of using a "rectangular" matrix $\mathbf{T}_2$ for transforming and reducing a dynamical system is a "specific characteristics" of the POG technique and it holds only for system described in the POG form (1). A simulative comparison between the extended model (4) of the planetary gear and the reduced model (7) is shown in Fig. 8. The parameters used in simulation are (SI units): sun parameters $[J_s,\, b_s,\, r_s] = [0.049,\, 4.946,\, 0.102]$; ring parameters $[J_r,\, b_r,\, r_r] = [2.180,\, 218.02,\, 0.248]$; carrier parameters $[J_c,\, b_c] = [0.929,\, 92.89]$; planet parameters $[J_p,\, b_p,\, r_p] = [0.081,\, 8.123,\, 0.073]$; stiffness parameters $[K_{sc},\, d_{sc}] = [K_{cr},\, d_{cr}] = [10^7,\, 10]$; initial conditions $[\omega_s(0),\, \omega_c(0),\, \omega_r(0)] = [0.1,\, -0.2,\, -0.323]$ rad/s; constant external torques $[\tau_s,\, \tau_c,\, \tau_r] = [0,\, 4,\, 0]$ Nm.

With different choices of matrix $\mathbf{T}_1$ it is possible to obtain different but equivalent reduced systems, similar to (7), with different state vectors $\mathbf{x}_1$, for example $\mathbf{x}_1 = \left[\,\omega_s,\, \omega_r\,\right]^{\mathrm{T}}$, $\mathbf{x}_1 = \left[\,\omega_r,\, \omega_c\,\right]^{\mathrm{T}}$, etc.

B. Reduced elastic model

Using the POG reduction technique it is also possible to obtain from (4) the reduced elastic model when inertias J_s, J_c and J_r go to zero. Applying to system (5) the following congruent transformation:

$$\overline{\mathbf{x}} = \mathbf{T}_3\,\mathbf{z}, \qquad \text{where} \qquad \mathbf{T}_3 = \begin{bmatrix} 0&0&0&1&0&0 \\ 1&0&0&0&0&0 \\ 0&1&0&0&0&0 \\ 0&0&0&0&1&0 \\ 0&0&1&0&0&0 \\ 0&0&0&0&0&1 \end{bmatrix}.$$

and using the constraint $J_s = J_c = J_r = 0$, one obtains the following transformed system:

$$\underbrace{\begin{bmatrix} \mathbf{L}_1 & 0 \\ 0 & 0 \end{bmatrix}}_{\mathbf{L}} \underbrace{\begin{bmatrix} \dot{\mathbf{z}}_1 \\ \dot{\mathbf{z}}_2 \end{bmatrix}}_{\dot{\mathbf{z}}} = \underbrace{\begin{bmatrix} \mathbf{A}_{11} & \mathbf{A}_{12} \\ \mathbf{A}_{21} & \mathbf{A}_{22} \end{bmatrix}}_{-\mathbf{A}} \underbrace{\begin{bmatrix} \mathbf{z}_1 \\ \mathbf{z}_2 \end{bmatrix}}_{\mathbf{z}} + \underbrace{\begin{bmatrix} \mathbf{B}_1 \\ \mathbf{B}_2 \end{bmatrix}}_{\mathbf{B}} \mathbf{u}, \quad \mathbf{y} = \mathbf{C}\,\mathbf{z} + \mathbf{D}\,\mathbf{u}, \tag{8}$$

where $\mathbf{z} = \mathbf{T}_1^{\mathrm{T}}\,\overline{\mathbf{x}}$, $\mathbf{L} = \mathbf{T}_3^{\mathrm{T}}\overline{\mathbf{L}}\,\mathbf{T}_3$, $\mathbf{A} = \mathbf{T}_3^{\mathrm{T}}\overline{\mathbf{A}}\,\mathbf{T}_3$, $\mathbf{B} = \mathbf{T}_3^{\mathrm{T}}\,\overline{\mathbf{B}}$, $\mathbf{C} = [\mathbf{C}_1,\ \mathbf{C}_2] = \mathbf{B}^{\mathrm{T}} = [\mathbf{B}_1^{\mathrm{T}},\ \mathbf{B}_2^{\mathrm{T}}]$, $\mathbf{D} = 0$ and where:

$$\mathbf{z}_1 = \begin{bmatrix} F_{sc} \\ \omega_p \\ F_{cr} \end{bmatrix}, \qquad \mathbf{z}_2 = \begin{bmatrix} \omega_s \\ \omega_c \\ \omega_r \end{bmatrix}, \qquad \mathbf{L}_1 = \begin{bmatrix} \frac{1}{K_{sc}} & 0 & 0 \\ 0 & J_p & 0 \\ 0 & 0 & \frac{1}{K_{cr}} \end{bmatrix},$$

$$\mathbf{A}_{11} = \begin{bmatrix} 0 & r_p & 0 \\ -r_p & -d_{sc}r_p^2 - r_p^2 d_{cr} - b_p & -r_p \\ 0 & r_p & 0 \end{bmatrix}, \qquad \mathbf{B}_1 = \begin{bmatrix} 0&0&0 \\ 0&0&0 \\ 0&0&0 \end{bmatrix},$$

$$\mathbf{A}_{12} = \begin{bmatrix} r_s & -r_s & 0 \\ -r_s d_{sc} r_p & r_s d_{sc} r_p - r_p r_r d_{cr} & r_p r_r d_{cr} \\ 0 & r_r & -r_r \end{bmatrix}, \ \mathbf{B}_2 = \begin{bmatrix} 1&0&0 \\ 0&1&0 \\ 0&0&1 \end{bmatrix},$$

$$\mathbf{A}_{21} = \begin{bmatrix} -r_s & -r_s d_{sc} r_p & 0 \\ r_s & r_s d_{sc} r_p - r_p r_r d_{cr} & -r_r \\ 0 & r_p r_r d_{cr} & r_r \end{bmatrix}, \qquad \mathbf{D} = \begin{bmatrix} 0&0&0 \\ 0&0&0 \\ 0&0&0 \end{bmatrix},$$

$$\mathbf{A}_{22} = \begin{bmatrix} -b_s - r_s^2 d_{sc} & r_s^2 d_{sc} & 0 \\ r_s^2 d_{sc} & -b_c - r_s^2 d_{sc} - r_r^2 d_{cr} & r_r^2 d_{cr} \\ 0 & r_r^2 d_{cr} & -b_r - r_r^2 d_{cr} \end{bmatrix}.$$

The last equation of system (8) shows the following algebraic relation between the state and input variables:

$$\mathbf{A}_{21}\,\mathbf{z}_1 + \mathbf{A}_{22}\,\mathbf{z}_2 + \mathbf{B}_2\,\mathbf{u} = 0$$

Since matrix $\mathbf{A}_{22}$ is invertible, vector $\mathbf{z}_2$ can be expressed as:

$$\mathbf{z}_2 = -\mathbf{A}_{22}^{-1}\mathbf{A}_{21}\,\mathbf{z}_1 - \mathbf{A}_{22}^{-1}\mathbf{B}_2\,\mathbf{u}$$

Applying the following rectangular transformation:

$$\mathbf{z} = \underbrace{\begin{bmatrix} \mathbf{I}_2 \\ -\mathbf{A}_{22}^{-1}\,\mathbf{A}_{21} \end{bmatrix}}_{\mathbf{T}_z}\,\mathbf{z}_1 + \underbrace{\begin{bmatrix} 0 \\ -\mathbf{A}_{22}^{-1}\,\mathbf{B}_2 \end{bmatrix}}_{\mathbf{T}_u}\,\mathbf{u}$$

to system (8) (i.e. $\mathbf{L}\,\dot{\mathbf{z}} = -\mathbf{A}\,\mathbf{z} + \mathbf{B}\,\mathbf{u}$ and $\mathbf{y} = \mathbf{C}\,\mathbf{z} + \mathbf{D}\,\mathbf{u}$), one obtains the following reduced system (note that $\mathbf{L}\,\mathbf{T}_u = 0$):

$$\begin{cases} \mathbf{T}_z^{\mathrm{T}}\mathbf{L}\,\mathbf{T}_z\,\dot{\mathbf{z}}_1 = -\mathbf{T}_z^{\mathrm{T}}\mathbf{A}\,\mathbf{T}_z\,\mathbf{z}_1 + \mathbf{T}_z^{\mathrm{T}}(\mathbf{B} - \mathbf{A}\,\mathbf{T}_u)\,\mathbf{u} \\ \mathbf{y} = \mathbf{C}\,\mathbf{T}_z\,\mathbf{z}_1 + (\mathbf{D} + \mathbf{C}\,\mathbf{T}_u)\,\mathbf{u} \end{cases}$$

that in compact form is:

$$\mathbf{L}_e\,\dot{\mathbf{z}}_1 = -\mathbf{A}_e\,\mathbf{z}_1 + \mathbf{B}_e\,\mathbf{u}, \qquad \mathbf{y} = \mathbf{C}_e^{\mathrm{T}}\mathbf{z}_1 + \mathbf{D}_e^{\mathrm{T}}\mathbf{u} \tag{10}$$

where matrices $\mathbf{L}_e$, $\mathbf{A}_e$, $\mathbf{B}_e$, $\mathbf{C}_e$ and $\mathbf{D}_e$ have the following structure:

$$\begin{aligned} \mathbf{L}_e &= \mathbf{T}_z^{\mathrm{T}}\mathbf{L}\,\mathbf{T}_z = \mathbf{L}_1, \\ -\mathbf{A}_e &= -\mathbf{T}_z^{\mathrm{T}}\mathbf{A}\,\mathbf{T}_z = \mathbf{A}_{11} - \mathbf{A}_{12}\,\mathbf{A}_{22}^{-1}\,\mathbf{A}_{21}, \\ \mathbf{B}_e &= \mathbf{T}_z^{\mathrm{T}}(\mathbf{B} - \mathbf{A}\,\mathbf{T}_u) = \mathbf{B}_1 - \mathbf{A}_{12}\,\mathbf{A}_{22}^{-1}\,\mathbf{B}_2, \\ \mathbf{C}_e &= \mathbf{C}\,\mathbf{T}_z = \mathbf{C}_1 - \mathbf{C}_2\,\mathbf{A}_{22}^{-1}\,\mathbf{A}_{21}, \\ \mathbf{D}_e &= \mathbf{D} + \mathbf{C}\,\mathbf{T}_u = \mathbf{D} - \mathbf{C}_2\,\mathbf{A}_{22}^{-1}\,\mathbf{B}_2. \end{aligned}$$

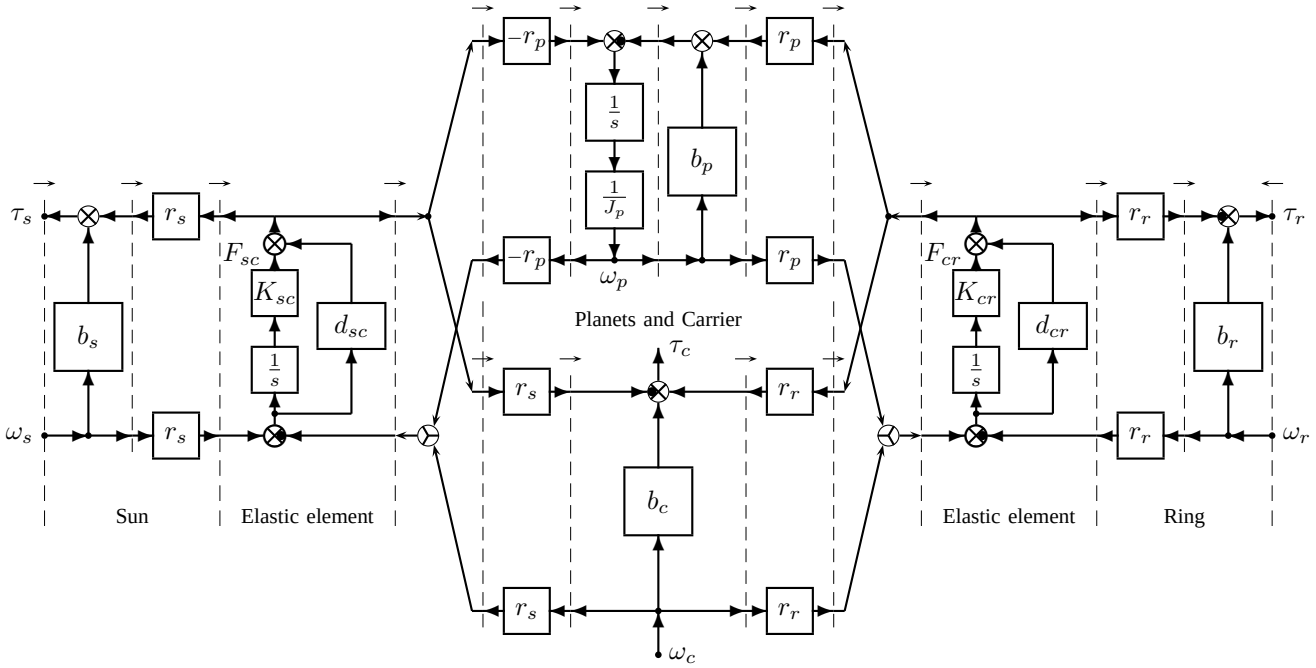

$$\underbrace{\begin{bmatrix} \frac{1}{K_{sc}} & 0 & 0 \\ 0 & J_p & 0 \\ 0 & 0 & \frac{1}{K_{cr}} \end{bmatrix}}_{\tilde{\mathbf{L}}_e} \underbrace{\begin{bmatrix} \dot{F}_{sc} \\ \dot{\omega}_p \\ \dot{F}_{cr} \end{bmatrix}}_{\dot{\tilde{\mathbf{x}}}} = \underbrace{\begin{bmatrix} 0 & r_p & 0 \\ -r_p & -r_p^2 d_{sc} - b_p - r_p^2 d_{cr} & -r_p \\ 0 & r_p & 0 \end{bmatrix}}_{-\tilde{\mathbf{A}}_e} \underbrace{\begin{bmatrix} F_{sc} \\ \omega_p \\ F_{cr} \end{bmatrix}}_{\tilde{\mathbf{x}}} + \underbrace{\begin{bmatrix} r_s & -r_s & 0 \\ -r_s d_{sc} r_p & r_s d_{sc} r_p - r_r d_{cr} r_p & r_r d_{cr} r_p \\ 0 & r_r & -r_r \end{bmatrix}}_{\tilde{\mathbf{B}}_e} \underbrace{\begin{bmatrix} \omega_s \\ \omega_c \\ \omega_r \end{bmatrix}}_{\tilde{\mathbf{u}}}$$

$$\underbrace{\begin{bmatrix} \tau_s \\ \tau_c \\ \tau_r \end{bmatrix}}_{\tilde{\mathbf{y}}} = \underbrace{\begin{bmatrix} r_s & r_s d_{sc} r_p & 0 \\ -r_s & -r_s d_{sc} r_p + r_r d_{cr} r_p & r_r \\ 0 & -r_r d_{cr} r_p & -r_r \end{bmatrix}}_{\tilde{\mathbf{C}}_e} \underbrace{\begin{bmatrix} F_{sc} \\ \omega_p \\ F_{cr} \end{bmatrix}}_{\tilde{\mathbf{x}}} + \underbrace{\begin{bmatrix} b_s + r_s^2 d_{sc} & -r_s^2 d_{sc} & 0 \\ -r_s^2 d_{sc} & b_c + r_s^2 d_{sc} + r_r^2 d_{cr} & -r_r^2 d_{cr} \\ 0 & -r_r^2 d_{cr} & b_r + r_r^2 d_{cr} \end{bmatrix}}_{\tilde{\mathbf{D}}_e} \underbrace{\begin{bmatrix} \omega_s \\ \omega_c \\ \omega_r \end{bmatrix}}_{\tilde{\mathbf{u}}} \tag{9}$$

Figure 9. POG block diagram and POG state space equations of the reduced planetary gear when $J_s = J_c = J_r = 0$ and the velocities are the inputs.

Since matrix $\mathbf{D}_e$ is invertible, system (10) can be input-output inverted using the relations shown in Fig. 5. The state space equations $\tilde{\mathbf{L}}_e\,\dot{\tilde{\mathbf{x}}} = -\tilde{\mathbf{A}}_e\,\tilde{\mathbf{x}} + \tilde{\mathbf{B}}_e\,\tilde{\mathbf{u}}$ and $\tilde{\mathbf{y}} = \tilde{\mathbf{C}}_e\,\tilde{\mathbf{x}} + \tilde{\mathbf{D}}_e\,\tilde{\mathbf{u}}$ of the inverted-reduced system are shown in (9) in the lower part of Fig. 9 where:

$$\tilde{\mathbf{L}}_e = \mathbf{L}_e,\quad \tilde{\mathbf{A}}_e = \mathbf{A}_e + \mathbf{B}_e\mathbf{D}_e^{-1}\mathbf{C}_e,\quad \tilde{\mathbf{B}}_e = \mathbf{B}_e\mathbf{D}_e^{-1},\quad \tilde{\mathbf{C}}_e = -\mathbf{D}_e^{-1}\mathbf{C}_e,$$

$$\tilde{\mathbf{x}} = \mathbf{z}_1,\quad \tilde{\mathbf{u}} = \mathbf{y} = [\omega_s, \omega_c, \omega_r]^{\mathrm{T}},\quad \tilde{\mathbf{y}} = \mathbf{u} = [\tau_s, \tau_c, \tau_r]^{\mathrm{T}},\quad \tilde{\mathbf{D}}_e = \mathbf{D}_e^{-1}.$$

A POG graphical representation of this inverted-reduced system is shown in the upper part of Fig. 9.

C. Reduced dissipative models

A first dissipative static model of the planetary gear can be obtained from the inertial model (7) when $J_s = J_c = J_p = J_r = 0$, that is when $\mathbf{L}_r = 0$:

$$\mathbf{x}_1 = \mathbf{A}_r^{-1}\,\mathbf{B}_r\,\mathbf{u}, \quad \rightarrow \quad \mathbf{y} = \mathbf{D}_{s1}\,\mathbf{u} = \mathbf{B}_r^{\mathrm{T}}\,\mathbf{A}_r^{-1}\,\mathbf{B}_r\,\mathbf{u}. \tag{11}$$

Matrix $\mathbf{D}_{s1}$ is singular and therefore all the torque vectors $\mathbf{u} = [\tau_s,\, \tau_c,\, \tau_r]^{\mathrm{T}}$ which belong to the kernel of matrix $\mathbf{B}_r$, i.e. which are parallel to vector $\mathbf{k}_1 = [r_s,\, -r_r - r_s,\, r_r]^{\mathrm{T}}$, do not influence the output velocities $\mathbf{y} = [\omega_s,\, \omega_c,\, \omega_r]^{\mathrm{T}}$. Moreover, all the velocities $\mathbf{y}$ obtained from (11) are perpendicular to vector $\mathbf{k}_1$, i.e. the vector $\mathbf{y}$ satisfies the relation:

$$\mathbf{k}_1^{\mathrm{T}}\,\mathbf{y} = 0 \quad \leftrightarrow \quad r_s\,\omega_s - (r_r + r_s)\,\omega_c + r_r\,\omega_r = 0. \tag{12}$$

A second dissipative static model can be obtained from the elastic model (10) when $K_{sc} = K_{sc} = \infty$ and $J_p = 0$, that is when $\tilde{\mathbf{L}}_e = 0$:

$$\tilde{\mathbf{A}}_e\,\tilde{\mathbf{x}} = \tilde{\mathbf{B}}_e\,\tilde{\mathbf{u}}, \qquad \tilde{\mathbf{y}} = \tilde{\mathbf{C}}_e\,\tilde{\mathbf{x}} + \tilde{\mathbf{D}}_e\,\tilde{\mathbf{u}}. \tag{13}$$

In this case a solution in closed form does not exists because matrix $\tilde{\mathbf{A}}_e$ is singular. One can easily verify that system (13) has a solution only when the input vector $\tilde{\mathbf{u}} = [\omega_s,\, \omega_c,\, \omega_r]^{\mathrm{T}}$ is perpendicular to vector $\mathbf{k}_1$, i.e. when $\mathbf{k}_1^{\mathrm{T}}\,\tilde{\mathbf{u}} = \mathbf{k}_1^{\mathrm{T}}\,\mathbf{y} = 0$ as shown in (12). So, the static dissipative model (13) cannot be used in practice because the input vector $\tilde{\mathbf{u}}$ is "constrained".

IV. POG MODELING OF AN HYBRID AUTOMOTIVE SYSTEM

It is well known, see for example [5], that the planetary gear is a key element for modeling hybrid automotive power structures. The hybrid structure shown in Fig. 10 includes an internal combustion engine (ICE), a multi-phase Permanent

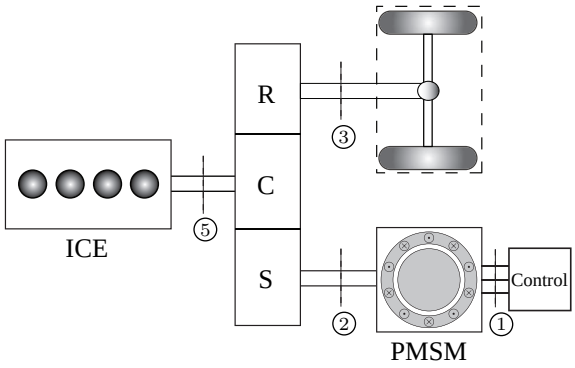

Figure 10. Scheme of the considered power structure of the vehicle

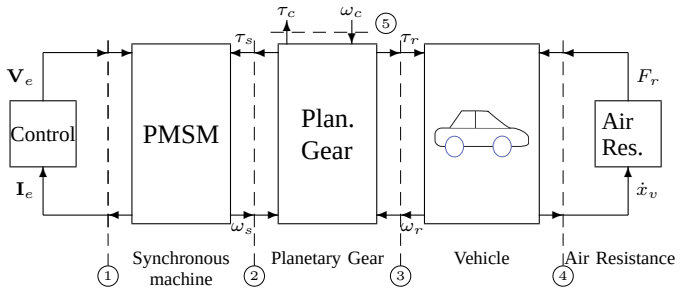

Figure 11. POG graphical representation of the considered hybrid vehicle.

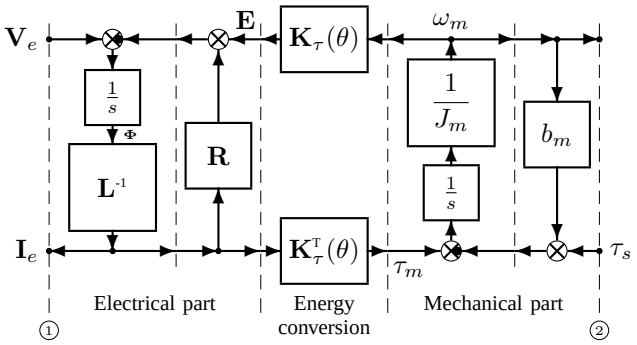

Figure 12. POG scheme of the multi-phase synchronous motor (PMSM).

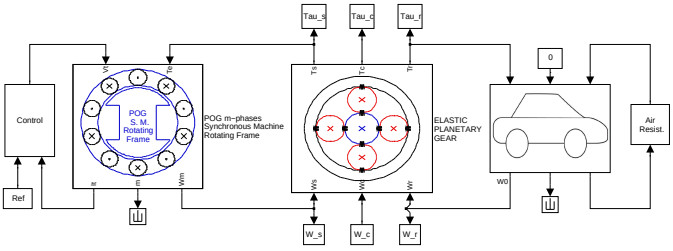

Figure 13. Simulink block scheme of the considered hybrid power structure.

Magnet Synchronous Machine (PMSM) and the vehicle. The planetary gear is the element connecting the two motors and the driving wheels. The ICE is rigidly connected to the Carrier (C), the PMSM is connected to the Sun (S) and the vehicle driving axle is connected to the Ring (R). This hybrid system can be dynamically described by the "high level" POG block scheme shown in Fig. 11. Note that the power sections ①-⑤ shown in Fig. 11 correspond to the physical power sections indicated in Fig. 10. The POG block "Control" of Fig. 11 represents the electric control of the PMSM. The POG model of the synchronous machine present between sections ① and ② is given in Fig. 12, see [6] and [7]. The POG model of the Planetary Gear present between sections ② and ③ is the elastic model given in Fig. 9. In ③ the planetary gear is connected to the driving shaft of the vehicle. The dynamics of the vehicle is described by the POG model present between sections ③ and ④: the details of this POG model can be found in [8]. Finally, the last POG block describes the resistance of the air F_r as a function of the vehicle velocity $\dot{x}_v$.

V. Simulation of the Hybrid Power Structure

The hybrid automotive system shown in Fig. 10 and Fig. 11 has been implemented in Matlab/Simulink. The obtained Simulink block scheme is shown in Fig. 13. All subsystems have been modeled with the POG technique and in particular the vehicle in the right part of the scheme is a bicycle model of a car that includes the tire-road elastic interaction, see [8].

The "start-and-stop" simulation results reported in Fig. 14÷18 have been obtained with the ICE switched off, i.e. $\omega_c = 0$, and controlling the multi-phase electric motor in order to force to the vehicle the start-and-stop longitudinal movement described by the trapezoidal velocity shape $\dot{x}_d$ shown in Fig. 14 (the red dashed line). The velocity $\dot{x}_v$ of the vehicle follows the desired velocity $\dot{x}_d$ with a small delay because of the elastic horizontal slipping of the tires on the ground. Main parameters of the vehicle: $M_v = 1272$ kg is the mass of the vehicle; $J_w = 3.459$ kg m^2 is the inertia of the wheels; $R_w = 32.55$ cm is the radius of the wheels; $K_t = 360000$ N/m is the longitudinal stiffness of the tires. The angular velocities of the planetary gear are shown in Fig. 15: sun ω_s (red, solid), carrier ω_c (blue, dashed) and ring ω_r (black, dash-dotted). Parameters of the planetary gear: $r_s = 10.2$ cm and $r_r = 24.8$ cm are the radii; $K_{sc} = K_{cr} = 10^7$ N/m and $d_{sc} = d_{cr} = 3003$ N s/m are the stiffness and friction coefficients; $J_p = 0.0812$ kg m^2 is the planet inertia; $[b_p, b_s, b_c, b_r] = [0.243, 0.148, 2.787, 6.541]$ N m/rad are the linear friction coefficients. The torques acting on the wheels of the planetary gear are shown in Fig. 16: sun τ_s (red, solid), carrier τ_c (blue, dashed) and ring τ_r (black, dash-dotted). The voltages $\mathbf{V}_e$ and the currents $\mathbf{I}_e$ of the m-phases electrical motor ($m = 5$) are shown in Fig. 17. Parameters of the multi-phase electric motor: the shape of the rotor flux is sinusoidal; the m phases are star connected; $R_s = 1\ \Omega$ and $L_s = 0.01$ H are the resistance and self inductance coefficient of the stator phases; $M_{s0} = 0.008$ H is the maximum value of mutual inductance between stator phases; $\varphi_c = 6$ W is the maximum value of the rotor flux chained with the stator phases; $J_m = 0.529$ kg m^2 and $b_m = 0.08$ N m s/rad are the inertia and the linear friction coefficient of the rotor. The main powers flowing through the sections of the system are shown in Fig. 18: P_1 (red,

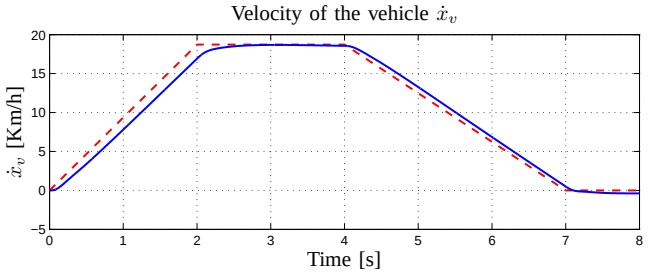

Figure 14. Velocity of the vehicle $\dot{x}_v$ (blue, solid) compared with the desired velocity $\dot{x}_d$ (red, dashed).

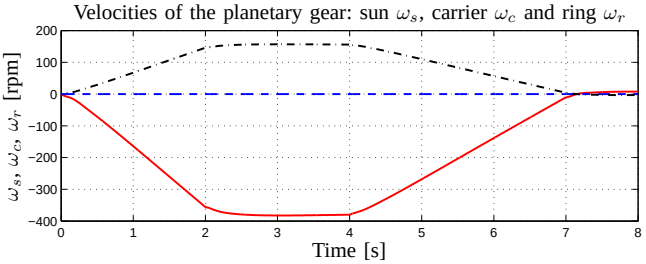

Figure 15. Velocities of the planetary gear: sun ω_s (red, solid), carrier ω_c (blue, dashed) and ring ω_r (black, dash-dotted).

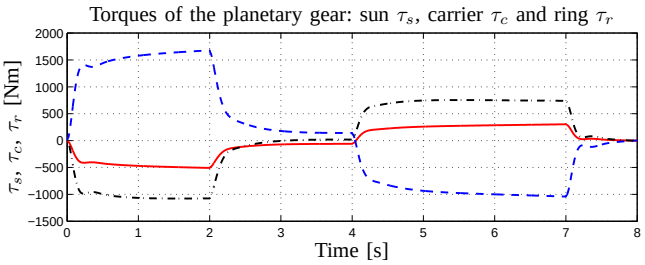

Figure 16. Torques within the planetary gear: sun τ_s (red, solid), carrier τ_c (blue, dashed) and ring τ_r (black, dash-dotted).

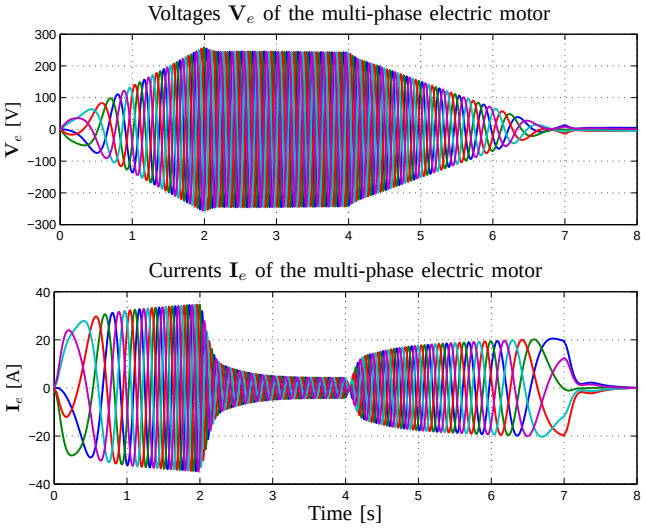

Figure 17. Phase voltages $\mathbf{V}_e$ and phase currents $\mathbf{I}_e$ of the multi-phase electric motor.

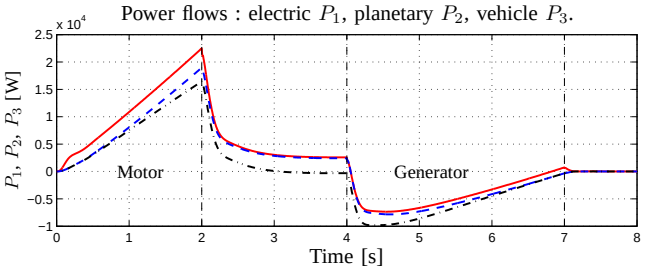

Figure 18. Powers entering the subsystems: P_1 electric motor (red, plain), P_2 planetary gear (blue, dashed), P_3 vehicle (black, dash-dotted).

plain) is the power in section ① flowing from the control unit towards the electric motor; P_2 (blue, dashed) is the mechanical power in section ② flowing from the electrical motor towards the planetary gear; P_3 (black, dash-dotted) is the mechanical power in section ③ which flows towards the vehicle. When $t \in [0, 2]$ s the vehicle accelerates and part of the power flowing towards the vehicle dissipates within the electric motor (i.e. the difference between the solid and dashed lines) and within the planetary gear (i.e. the difference between the dashed and dash-dotted lines). When $t \in [4, 7]$ s the vehicle decelerates and a consistent amount of mechanical power flows from the vehicle towards the electric motor: in this phase the motor acts as a generator, see Fig. 18.

VI. Conclusions

In this paper a planetary gear has been modeled with different level of details using the Power-Oriented Graphs (POG) technique. POG congruent state space transformations have been used to obtain the reduced models when the elasticities and/or the inertias of the system go to zero. A full hybrid automotive power system (endothermic engine, multi-phase synchronous motor, planetary gear and vehicle dynamics) has been modeled using POG. The final simulations results clearly show that the POG technique is also suitable to easily, clearly and precisely model complex dynamic systems.

References

[1] R. Zanasi, "Power Oriented Modelling of Dynamical System for Simulation", IMACS Symp. on Modelling and Control of Technological System, Lille, France, May 1991.

[2] Zanasi R., "Dynamics of a n-links Manipulator by Using Power-Oriented Graph", *SYROCO '94*, Capri, Italy, 1994.

[3] Paynter, H.M., *Analysis and Design of Engineering Systems*, MIT-press, Camb., MA, 1961.

[4] D. C. Karnopp, D.L. Margolis, R. C. Rosemberg, *System dynamics - Modeling and Simulation of Mechatronic Systems*, Wiley Interscience, ISBN 0-471-33301-8, 3rd ed. 2000.

[5] Miller, J.M., "Hybrid Electric Vehicle Propulsion System Architectures of the e-CVT Type, IEEE Transactions On Power Electronics, Vol. 21, No. 3, May 2006.

[6] R. Zanasi, F. Grossi, "Multi-phase Synchronous Motors: POG Modeling and Optimal Shaping of the Rotor Flux", ELECTRIMACS 2008, Québec, Canada, June 2008.

[7] R. Zanasi, F. Grossi "Optimal Rotor Flux Shape for Multi-phase Permanent Magnet Synchronous Motors", International Power Electronics and Motion Control Conference, September 1-3 2008, Poznan, Poland.

[8] F. Grossi, W. Lhomme, R. Zanasi, A. Bouscayrol, "Modelling and control of a vehicle with tire-road interaction using POG and EMR formalisms", accepted to Electromotion 2009, EPE chapter Electric Drives, 1-3 July 2009, Lille, France